

ELASTOPLASTIC STATE OF FLEXIBLE CYLINDRICAL SHELLS WITH A CIRCULAR HOLE UNDER AXIAL TENSION

I. S. Chernyshenko, E. A. Storozhuk, and S. B. Kharenko

UDC 539.374

The elastoplastic state of cylindrical shells with a circular hole is studied considering finite deflections. The material of the shells is isotropic and homogeneous; the load is axial tension. The distribution of stresses, strains, and displacements along the hole boundary and in the zone of their concentration is studied by solving a doubly nonlinear problem. The data obtained are compared with the solutions of the physically and geometrically nonlinear problems and a numerical solution of the linear elastic problem

Keywords: doubly nonlinear problem, cylindrical shell, stress concentration, circular hole, axial tension, plastic strain, finite deflection

Introduction. Using the real properties of structural materials in creating various thin-walled structures and their elements (shells or plates) is one of the basic lines of development of modern engineering. Such elements made of modern metal and composite materials often have complicated shape (geometry), which includes stress concentrators (holes, cutouts, inclusions, and joints) [1, 3–5, 12]. Therefore, it is important to examine the influence of the properties of materials and the way they deform on the stress (strain or displacement) fields near holes under static loads of high levels.

It should be noted that the publications [2, 4, 6, 7, etc.] are concerned with the statement and solution of certain classes of nonlinear problems for thin shells with stress concentrators under surface and boundary loads of high levels, with the nonlinear properties of structural materials and large (finite) deflections taken into account. A generalized procedure for numerical solution of physically and geometrically nonlinear problems for arbitrary thin-walled shells made of metals and occupying simply and multiply connected domains is presented in the paper [2], which gives a generalized statement of nonlinear problems that allows for the shape of shells and holes, the type and stage of loading, and features of the algorithm and associated software. The publications [8–11] present numerical solutions to two-dimensional (nonaxisymmetric) nonlinear problems for flexible spherical, cylindrical, and conical shells under surface pressure. Numerical data for shells subject to axial forces are reported in [4, 7, 13].

Expanding upon [8, 9], the present paper discusses results on the elastoplastic stress–strain state around a curvilinear (circular) hole in flexible cylindrical shells under axial tension. We will examine the combined effect of nonlinear factors (plastic strains and finite deflections) on the distribution of stresses, strains, and displacements along and near the boundary of the hole for certain geometrical and material characteristics.

1. We will analyze the stress–strain state around a curvilinear (circular) hole in a thin cylindrical shell subjected to axial tensile forces $P = \text{const}$ uniformly distributed along the edges of the shell (Fig. 1). The shell is made of an isotropic material (metal) (see [1, 4] for its physical and mechanical characteristics and stress–strain curves (σ versus ε) and (σ_i versus ε_i)). It is assumed that a high-level load causes plastic strains and large (finite) deflections comparable with the thickness of the shell [2, 4].

The nonlinear governing equations can be derived using the geometrically nonlinear relations of the theory of deep thin shells based on the Kirchhoff–Love hypotheses (geometrically nonlinear theory of shells of the second order [4, 7]) and the physically nonlinear relations based on the theory of flow with isotropic hardening (von Mises yield criterion and associated

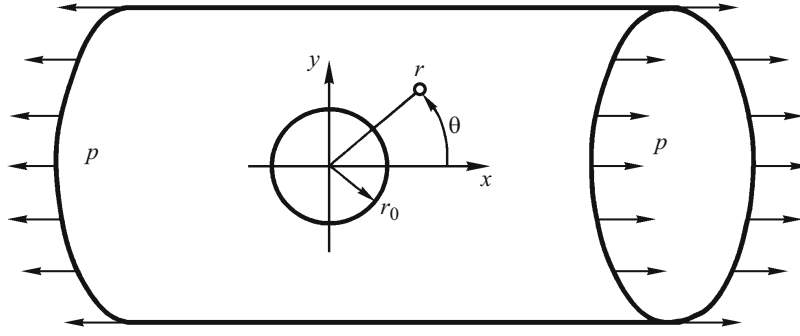


Fig. 1

flow rule). In the case of simple (or nearly simple) loading, use is usually made of nonlinear constitutive equations [2, 4], which are derived using the theory of small elastoplastic deformation where the coefficient of transverse deformation beyond the elastic limit is variable.

Let us consider a flexible cylindrical shell of radius R and thickness h with a hole of radius r_0 under axial forces $P = P_0 / h \cdot 10^3$ Pa. Some boundary conditions are prescribed at the edges of the hole. The mid-surface of the shell is described in a rectangular Cartesian coordinate system (x, y) , while its geometry in a global Cartesian coordinate system (X, Y, Z) (Fig. 1) with the OX -axis aligned with the shell axis and the OZ -axis passing through the center of the hole.

The nonlinear kinematic equations can be written for the mid-surface:

$$\begin{aligned} \varepsilon_{xx} &= \frac{\partial u}{\partial x} + \frac{1}{2} \theta_1^2, & \varepsilon_{yy} &= \frac{\partial v}{\partial y} + \frac{1}{R} w + \frac{1}{2} \theta_2^2, & \varepsilon_{xy} &= \frac{\partial u}{\partial y} + \frac{\partial v}{\partial x} + \theta_1 \cdot \theta_2, \\ \alpha_{xx} &= \frac{\partial \theta_1}{\partial x}, & \alpha_{yy} &= \frac{\partial \theta_2}{\partial y}, & 2\alpha_{xy} &= \frac{\partial \theta_1}{\partial y} + \frac{\partial \theta_2}{\partial x}, & \theta_1 &= -\frac{\partial w}{\partial x}, & \theta_2 &= -\frac{\partial w}{\partial y} + \frac{1}{R} v. \end{aligned} \quad (1)$$

At the active stage of deformation (simple loading), the nonlinear constitutive equations can be represented in the following form [2, 4]:

$$\sigma_{xx} = \frac{2G}{1-\nu} (e_{xx} + \nu e_{yy}) + \sigma_{xx}^* \quad (x \leftrightarrow y), \quad \sigma_{xy} = G e_{xy} + \sigma_{xy}^*, \quad (2)$$

where σ_{xx}^* , σ_{yy}^* , and σ_{xy}^* are nonlinear terms defined by the following formulas, according to the theory of small elastoplastic deformation:

$$\begin{aligned} \sigma_{xx}^* &= -\frac{2}{3} \frac{G}{1-\nu} \omega_i [(2-\nu)e_{xx} - (1-2\nu)e_{yy} + (1+\nu)e_{zz}] \quad (x \leftrightarrow y), \\ \sigma_{xy}^* &= -G \omega_i e_{xy}, \end{aligned} \quad (3)$$

where

$$\begin{aligned} e_{xx} &= \varepsilon_{xx} + z\alpha_{xx} \quad (x \leftrightarrow y), & e_{xy} &= \varepsilon_{xy} + 2z\alpha_{xy}, & e_{zz} &= -\mu_i (e_{xx} + e_{yy}), \\ \omega_i &= 1 - \frac{\sigma_i}{3Ge_i}, & \mu_i &= -\frac{3\nu + (1-2\nu)\omega_i}{3(1-\nu) - 2(1-2\nu)\omega_i}, \end{aligned} \quad (4)$$

where ω_i is a plasticity function; σ_i and e_i are the stress and strain intensities; G and ν are the shear modulus and Poisson's ratio; the symbol (\leftrightarrow) denotes permutation of the indices.

In the theory of flow with isotropic hardening (combined loading), the nonlinear constitutive equations relate the stress vector $\{\sigma\}$ and the strain vector $\{e\}$ as follows (in vector-matrix form) [2, 4]:

$$\begin{aligned}\{\sigma\} &= [D](\{e\} - \{e^p\}) = [D]\{e\} + \{\sigma^p\} = [D]\{e^0\} + \{\sigma^n\}, \\ \{\sigma^p\} &= -[D]\{e^p\}, \quad \{\sigma^n\} = [D]\{e^n\} + \{\sigma^p\}.\end{aligned}\quad (5)$$

Denoting the displacement vectors and angles of rotation as

$$\{U\} = \{u, v, w\}^T, \quad \{\theta\} = \{\theta_1, \theta_2\}^T \quad (6)$$

and considering that

$$\{e\} = \{e_{xx}, e_{yy}, e_{xy}\}^T = \{\varepsilon\} + z\{\kappa\} = \{e^0\} + \{e^n\}, \quad (7)$$

we obtain the following equalities for the linear and nonlinear components of the strain vector:

$$\{e^0\} = [A_\varepsilon]\{U\} + z[A_\kappa]\{\theta\}, \quad \{e^n\} = \frac{1}{2}[A_L]\{\theta\}, \quad \{\theta\} = [A_\theta]\{U\}, \quad (8)$$

where $[A_\varepsilon]$, $[A_\kappa]$, and $[A_\theta]$ are matrices of linear differentiation operations; and $[A_L]$ is the matrix of angles of rotation θ_1 and θ_2 .

2. To derive the governing equations describing the elastoplastic state of a cylindrical shell with a curvilinear hole subject to finite deflections and to develop methods for approximate solution of nonlinear problems, we use the incremental-loading procedure and the nonlinear relations (1), (2) or (5)–(8) and governing equations in incremental form.

In the general case of arbitrary thin shells described in coordinates not aligned with the lines of principal curvatures, these relations and governing equations are represented in matrix form. This system was derived in [2] using the virtual-displacement principle, the modified Newton–Kantorovich method, the method of additional stresses, and a modified finite-element method.

The final system of governing algebraic equations follows from the stationarity conditions for the linearized total energy of the shell. At the n th step of loading, the system has the form

$$[S]\{\Delta q\} = \{\Delta V\}, \quad (9)$$

where $[S] = [S_0] + [S_\alpha] + [S_\sigma]$, $\{\Delta V\} = \{\Delta R\} - \{\Delta N\} + \{\Delta \Phi\}$, where $[S_0]$ is the stiffness matrix for linear elastic shells, $[S_\alpha]$ and $[S_\sigma]$ are the influence matrices of the initial angles of rotation θ_1 and θ_2 and stresses, respectively; $\{\Delta q\}$ is the column vector of displacements of nodal degrees of freedom (nodal unknowns); $\{\Delta R\}$, $\{\Delta N\}$, and $\{\Delta \Phi\}$ are the vectors of loads, nonlinearities, and residuals of the equilibrium equations at the end of the $(n - 1)$ th step of loading.

In solving specific boundary-value problems for shells, Eqs. (9) should be supplemented with boundary conditions at the external and internal edges.

We will use the following boundary conditions:

(a) free-edge conditions for the hole [4]:

$$\tilde{T}_r = \tilde{T}_{r\theta} = 0, \quad M_r = 0, \quad \tilde{Q}_r^* = 0, \quad (10)$$

(b) symmetry conditions on the boundaries $x = 0$ ($y = 0$):

$$u_y = 0, \quad \theta_y = 0, \quad \tilde{T}_{xy} = 0, \quad \tilde{Q}_y^* = 0 \quad (y \rightarrow x), \quad (11)$$

(c) membrane deflection and zero forces and moment on the boundary $y = y_k$:

$$w = -\frac{\nu PR}{Eh}, \quad \tilde{T}_y = \tilde{T}_{xy} = 0, \quad M_y = 0, \quad (12)$$

(d) membrane stress on the boundary $x = x_k$

$$M_x = 0, \quad \tilde{T}_{xy} = \tilde{Q}_y^* = 0, \quad \tilde{T}_x = P. \quad (13)$$

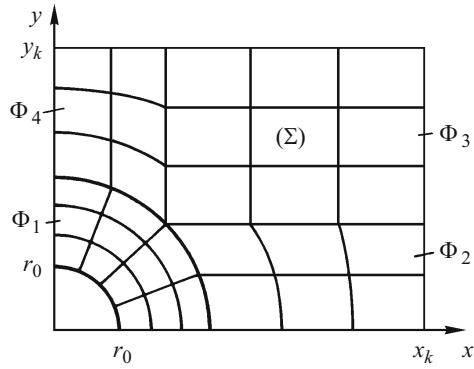


Fig. 2

TABLE 1

θ	ς	$e_r \cdot 10^2$			
		LP	PNP	GNP	PGNP
0	0.5	0.0117	-0.0254	-0.0009	-0.0353
	-0.5	0.1214	0.2229	0.0986	0.1513
$\pi/7$	0.5	-0.0096	-0.0341	-0.0042	-0.0096
	-0.5	0.0742	0.1804	0.0256	0.0419
$\pi/4$	0.5	-0.0601	-0.1127	-0.0562	-0.0492
	-0.5	-0.0425	0.0875	-0.0644	-0.0400
$5\pi/14$	0.5	-0.1276	-0.4679	-0.1312	-0.2225
	-0.5	-0.1646	-0.2217	-0.1447	-0.3661
$\pi/2$	0.5	-0.1794	-0.9510	-0.1833	-0.7376
	-0.5	-0.2636	-0.1569	-0.1937	-0.7518

TABLE 2

θ	ς	$e_\theta \cdot 10^2$			
		LP	PNP	GNP	PGNP
0	0.5	-0.0215	0.0962	0.0197	0.1186
	-0.5	-0.4026	-0.6189	-0.3265	-0.4392
$\pi/7$	0.5	0.0415	0.1182	0.0180	0.0395
	-0.5	-0.2470	-0.5211	-0.0824	-0.1329
$\pi/4$	0.5	0.1995	0.3266	0.1842	0.1680
	-0.5	0.1020	-0.2440	0.2165	0.1461
$5\pi/14$	0.5	0.4153	1.1050	0.4320	0.7848
	-0.5	0.5464	0.6086	0.4808	0.8710
$\pi/2$	0.5	0.5820	1.9200	0.6046	1.6410
	-0.5	0.8745	3.6370	0.6412	1.6800

TABLE 3

θ	ς	σ_{θ}^0			
		LP	PNP	GNP	PGNP
0	0.5	-138	682	149	831
	-0.5	-2817	-1805	-2284	-1673
$\pi/7$	0.5	297	831	129	282
	-0.5	-1728	-1705	-575	-926
$\pi/4$	0.5	1396	1395	1287	995
	-0.5	713	-1188	1517	896
$5\pi/14$	0.5	2900	1836	3020	1808
	-0.5	3823	1634	3364	1847
$\pi/2$	0.5	4063	1976	4228	1986
	-0.5	6119	2399	4485	1995

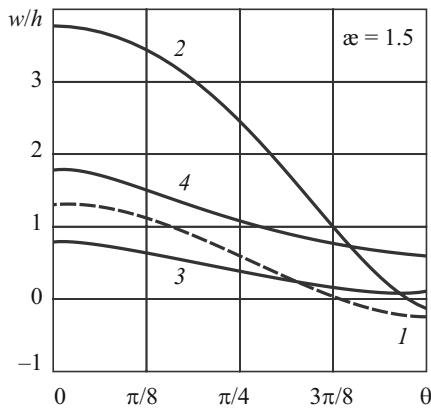


Fig. 3

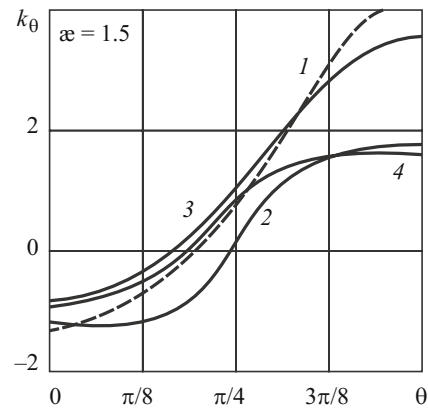


Fig. 4

To construct a design model for the shell, we consider the domain (Σ) of the mid-surface bounded by the lines $x = 0$, $x = x_k$, $y = 0$, and $y = y_k$ and the boundary of the hole (Fig. 2). Next we partition the domain (Σ) into four fragments Φ_i ($i = 1..4$) to divide them into quadrangular finite elements (FEs) of sizes 7×14 , 7×7 , 7×7 , and 7×7 , respectively. The internal and external boundaries of the first fragment are circles of radii $r = r_0$ and $r = 2r_0$, and the other lines that fragment the domain (Σ) are straight.

3. The numerical results to be discussed below have been obtained for a cylindrical shell with the following geometrical parameters (Fig. 1): $\eta = R / h = 400$, $\rho = r_0 / h = 30$ ($\alpha = r_0 / \sqrt{Rh} = 1.5$) ($x_k = y_k = 6r_0$). The shell is subject to axial forces $P_0 / h = 1200$ and is made of AMg-6 alloy with the following characteristics: $E = 70$ GPa; $\nu = 0.3-0.5$; $\sigma_n = 140$ MPa; $\epsilon_n = 0.002$; $\sigma_T = 165$ MPa.

We used Eqs. (9) with the boundary conditions (10)–(13). The loading process was divided into ten steps.

We used the developed method and associated software [2] to analyze the stress–strain state of this shell with allowance for plastic strains and large (finite) deflections. Some of the numerical results are presented in the tables and figures below.

TABLE 4

r/r_0	ξ	σ_θ^0			
		LP	PNP	GNP	PGNP
1	0.5	4063	1976	4228	1986
	-0.5	6119	2399	4485	1995
$1\frac{4}{7}$	0.5	1229	1318	1766	1878
	-0.5	2684	2168	2141	1975
$2\frac{4}{7}$	0.5	955	1034	1208	1442
	-0.5	1514	1756	1448	1617
$3\frac{5}{7}$	0.5	1073	1115	1155	1292
	-0.5	1172	1445	1229	1446
$4\frac{6}{7}$	0.5	1130	998	1131	1090
	-0.5	1143	1106	1142	1134
6	0.5	1212	1174	1186	1163
	-0.5	1212	1174	1186	1163

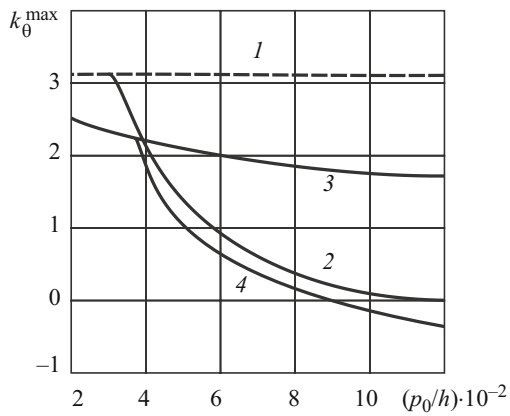


Fig. 5

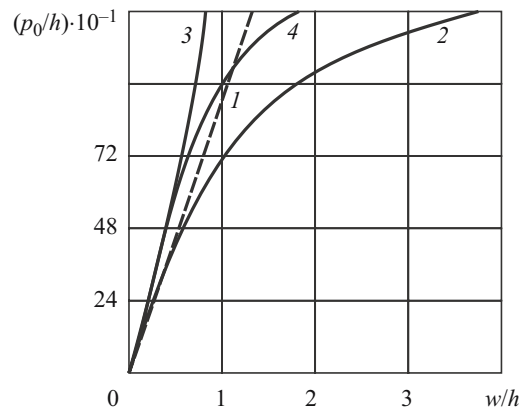


Fig. 6

Tables 1–3 summarize the strains (e_r, e_θ) and stresses $\sigma_\theta = \sigma_\theta^0 \cdot 10^5$ Pa on the outside and inside ($\xi = z/h = \pm 0.5$) surfaces of the shell on the boundary of the hole ($0 \leq \theta \leq \pi/2$) obtained considering the nonlinear material properties and large deflections (PGNP).

For comparison, the tables include the solutions of the linear elastic problem (LP), the physically nonlinear problem (PNP), and the geometrically nonlinear problem (GNP). Table 4 gives the hoop stresses σ_θ^0 along the radial cross section ($r_0 \leq r \leq 6r_0, \theta = \pi/2$).

Figures 3 and 4 show the variation in the relative deflection ($w^* = w/h$) and the concentration factor for membrane hoop stresses ($K_\theta = \sigma_\theta h/P$) along the boundary of the hole for the LP (curve 1), PNP (curve 2), GNP (curve 3), and PGNP (curve 4). Analyzing these results, we conclude that when a cylindrical shell with a circular hole is subjected to axial tension, the

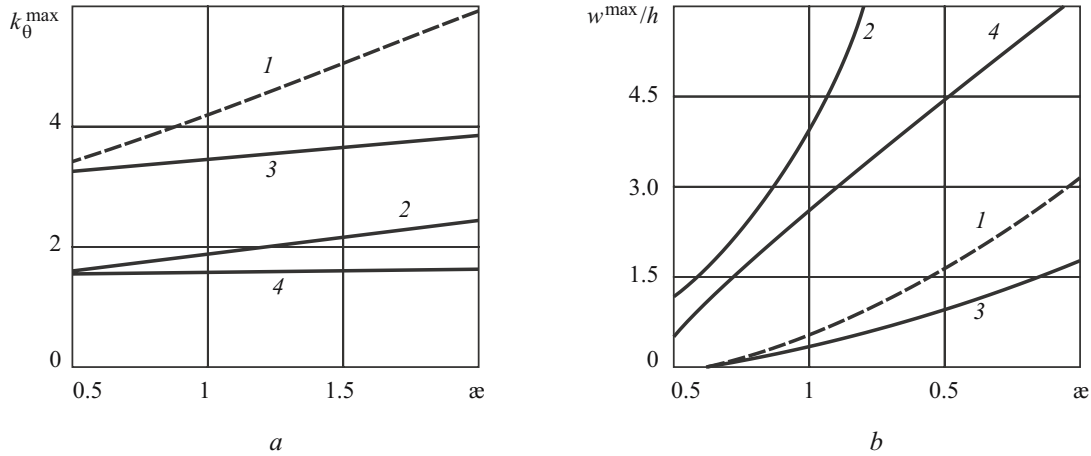


Fig. 7

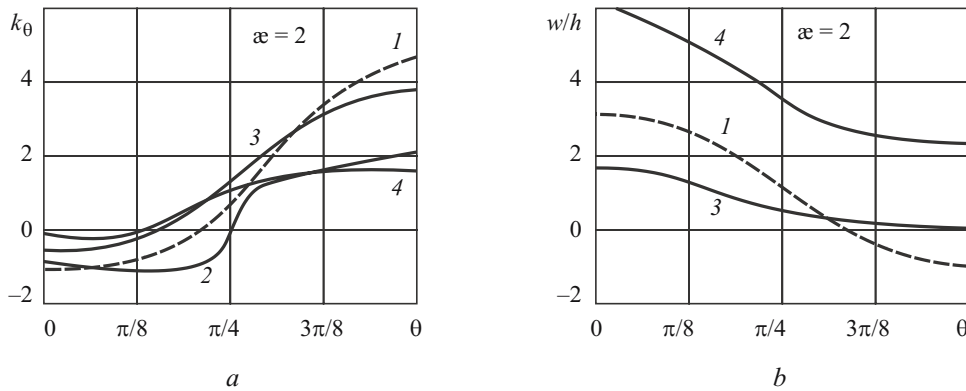


Fig. 8

most critical point is the one with the coordinates $r = r_0, \theta = \pi/2$ on the inside surface, where the stresses σ_θ and strains e_θ are maximum. As is seen in Fig. 3, the displacement w is maximum at the point $(r = r_0, \theta = 0)$ on the boundary of the hole.

Plastic strains equalize stresses in the most critical section $(r = r_0, \theta = \pi/2)$, decrease the maximum stress by 61%, and increase the maximum deflections and strains by 2.85 and 4.16, respectively, compared with those in the LP.

Comparing and analyzing the data in Tables 1–3 and Fig. 3, we see that the maximum stresses, strains, and deflections obtained in the GNP decrease by 27, 27, and 37%, respectively, compared with the LP. Large (finite) deflections equalize the stresses and strains in sections where they are maximum.

Plastic strains and finite deflections together decrease the maximum stresses by 67, 17, and 56% compared with the LP, PNP, and GNP, respectively. Finite deflections also have a substantial effect on the strain state of the shell during the elastoplastic stage of deformation. For example, the maximum deflections and strains in the PGNP differ from those in the LP, PNP, and GNP by 35, 53, 116% and 92, 54, 162%. When both physical and geometrical nonlinearities are taken into account, the stresses and strains in the most critical sections are redistributed and equalized throughout the thickness.

4. Let us analyze the variation in the stress–strain state around a hole in a shell (its geometrical and material characteristics are specified above) with increase in the load $(0 < P_0 / h \leq 1200)$. Figures 5 and 6 show the maximum stress concentration factor K_θ and the maximum relative deflection in the shell as functions of the applied forces (axial tension).

These results suggest that the shell deforms elastically when $0 < P_0 < 300$ in the PNP and $0 < P_0 / h < 350$ in the PGNP and plastically when $P_0 / h > 300$ in the PNP and $P_0 / h > 350$ in the PGNP. As the axial force increases, K_θ decreases and the plastic zone around the hole shifts in the meridional direction. In this case, $K_\theta = 5.1$ in the LP, and $K_\theta = 4.5, 4.2, 4.1$ for $P_0 / h = 360$ and $K_\theta = 2.0, 3.7, 1.7$ for $P_0 / h = 1200$ in the PNP, GNP, PGNP.

5. Let us examine the influence of the geometrical parameter $(\alpha = r_0 / \sqrt{Rh})$ on the elastoplastic state of a flexible cylindrical shell with a circular hole under tensile force $P_0 / h = 1500$. The parameter α varies from 0.2 to 2.

Figures 7 and 8 show the maximum stress concentration factor $K_{\theta}^{\max} = \sigma_{\theta}^{\max} h / P$ and the maximum relative deflection $w^{*\max} = w^{\max} / h$ as functions of α . Figure 8 shows how K_{θ} and $w^{*} = w / h$ vary along the boundary of the hole for the maximum value of the geometrical parameter ($\alpha = 2$).

Analyzing these data, we conclude that for all values of the parameter, the stresses (σ_{θ}) and strains (e_{θ}) peak at the point ($r = r_0, \theta = \pi / 2$) on the boundary of the hole on the inside surface of the shell ($\xi = -0.5$), while the deflections are maximum at the point ($r = r_0, \theta = 0$). The exception is the deflections for $\alpha = 0.5$ in the LP and GNP. They peak at the point ($r = r_0, \theta = \pi / 2$). It can be seen from Fig. 7a that as the parameter α increases, K_{θ} increases from $K_{\theta} = 3.44$ for $\alpha = 0.5$ to $K_{\theta} = 5.86$ for $\alpha = 2$ in the LP, from $K_{\theta} = 1.63$ for $\alpha = 0.5$ to $K_{\theta} = 2.44$ for $\alpha = 2$ in the PNP, from $K_{\theta} = 3.30$ for $\alpha = 0.5$ to $K_{\theta} = 3.85$ for $\alpha = 2$ in the GNP, and from $K_{\theta} = 1.57$ for $\alpha = 0.5$ to $K_{\theta} = 1.64$ for $\alpha = 2$ in the PGNP.

Note that this method discussed here can also be used to analyze the stress–strain state states of cylindrical and conical shells with an elliptic hole under tensile forces.

REFERENCES

1. A. N. Guz, A. G. Makarenkov, and I. S. Chernyshenko, *Structural Strength of Solid Propellant Engines* [in Russian], Mashinostroenie, Moscow (1980).
2. A. N. Guz, E. A. Storozhuk, and I. S. Chernyshenko, “Physically and geometrically nonlinear static problems for thin-walled multiply connected shells,” *Int. Appl. Mech.*, **39**, No. 6, 679–687 (2003).
3. A. V. Karmishin, V. A. Lyaskovets, V. N. Myachenkov, and A. N. Frolov, *Statics and Dynamics of Thin-Walled Shell Structures* [in Russian], Mashinostroenie, Moscow (1975).
4. A. N. Guz, I. S. Chernyshenko, V. N. Chekhov, et al., *Theory of Thin Shells Weakened by Holes*, Vol. 1 of the five-volume series *Methods of Shell Design* [in Russian], Naukova Dumka, Kyiv (1980).
5. A. N. Guz, A. S. Kosmodamianskii, V. P. Shevchenko, et al., *Stress Concentration*, Vol. 7 of the 12-volume series *Mechanics of Composite Materials* [in Russian], A.S.K., Kyiv (1998).
6. E. A. Storozhuk, “Two-dimensional elastoplastic problems in the theory of flexible shells with curvilinear holes,” *Int. Appl. Mech.*, **31**, No. 5, 355–359 (1995).
7. A. P. Shapovalov, “Effect of circular unreinforced holes on the stability of axially loaded cylindrical shells in the elasticoplastic zone,” *Strength of Materials*, **6**, No. 5, 638–643 (1974).
8. I. S. Chernyshenko and E. A. Storozhuk, “Inelastic deformation of flexible cylindrical shells with a curvilinear hole,” *Int. Appl. Mech.*, **42**, No. 12, 1414–1420 (2006).
9. I. S. Chernyshenko, E. A. Storozhuk, and F. D. Kadyrov, “Inelastic deformation of flexible cylindrical shells with an elliptic hole,” *Int. Appl. Mech.*, **43**, No. 5, 512–518 (2007).
10. I. S. Chernyshenko, E. A. Storozhuk, and S. B. Kharenko, “Physically and geometrically nonlinear deformation of thin-walled conical shells with a curvilinear hole,” *Int. Appl. Mech.*, **43**, No. 4, 418–424 (2007).
11. I. S. Chernyshenko, E. A. Storozhuk, and I. B. Rudenko, “Stress–strain state of a flexible spherical shell with an eccentric circular hole,” *Int. Appl. Mech.*, **43**, No. 10, 1142–1148 (2007).
12. A. N. Guz, I. S. Chernyshenko, and K. I. Shnerenko, “Stress concentration near openings in composite shells,” *Int. Appl. Mech.*, **37**, No. 2, 139–181 (2001).
13. E. A. Storozhuk and I. S. Chernyshenko, “Elastoplastic deformation of flexible cylindrical shells with two circular holes under axial tension,” *Int. Appl. Mech.*, **41**, No. 5, 506–511 (2005).